25th ABCM International Congress of Mechanical Engineering
October 20-25, 2019, Uberlândia, MG, Brazil

COB-2019-1549
A COMPARISON OF HYBRID URANS-LES TURBULENCE MODELS FOR THE COMPUTATION OF THE FLOW AROUND A TRIANGULAR BLUFF BODY

Alex José Elias
Aristeu da Silveira Neto
João Marcelo Vedovoto
Universidade Federal de Uberlândia
alex.elias@ufu.br, aristeus@ufu.br, vedovoto@ufu.br

Abstract. *This paper presents a comparison of Large Eddy Simulation (LES) and Unsteady Reynolds-Averaged Navier-Stokes (URANS) based on the Spalart-Allmaras (SA) turbulence closure model versus two hybrid URANS-LES methodologies, also based on the SA model: the Detached-Eddy Simulation (SA-DES) and Scale-Adaptive Simulation (SA-SAS). The hybrid methodologies were implemented in the MFSim code, developed in the Laboratório de Mecânica dos Fluidos of the Universidade Federal de Uberlândia in partnership with PETROBRAS. The models performance were assessed in the Volvo burner, wich features the canonical configuration of a bluff-body stabilized premixed flame. The studies on this configuration were carried out experimentally under the Volvo Flygmotor AB program. In order to compare the different turbulent closure models, only the non-reacting case is considered in this study. The benefits of this selection are twofold: it allows us to ignore the combustion, while it presents a characteristic vortex shedding in the wake behind the bluff body, which is interesting to perform the models comparison. Despite the observed necessity of a better description of the turbulence at the domain inlet, results from all models show good agreement with experimental data. In particular, the SA-SAS model presents great potential of use within the MFSim code, since it does not have explicit dependence of the computational mesh like LES and DES models.*

Keywords: *hybrid URANS-LES, DES, SAS, Bluff body*

1. INTRODUCTION

Most of the flows occurring in nature are turbulent. The same can be said about flows of industrial interest. Thus, the differential mathematical modeling of fluid flows enables us to better understand the physical phenomena involved in its occurrence, while providing a large number of valuable information, which are difficult to obtain through material experiments. For this reason, the scientific community has been engaged over the years in developing new modeling strategies for turbulent flows. Particularly over the past decade, hybrid URANS-LES modelling approaches have received increasing attention from the turbulence-research community (Haase *et al.*, 2009). This attention is justified once hybrid URANS-LES models are potentially more computationally efficient than Large Eddy Simulation (LES) and more accurate than Unsteady Reynolds-Averaged Navier-Stokes (URANS) (Peng *et al.*, 2010).

The first hybrid URANS-LES model was introduced by Spalart *et al.* (1997). The so-called Detached Eddy Simulation (DES) was based on a formulation of the Spalart-Allmaras (1994) turbulence model. Spalart proposed that the "attached" boundary eddies should be modelled in the URANS mode, while the larger "detached" eddies shoud be simulated. Latter on, numerous works were carried out in order to attest the quality of the DES, extending the Spalart proposal to other URANS models, providing impressive results for complex aerodynamic applications. An issue that was continuously investigated concerns the explicitly dependence of the mesh size in DES models. It was observed that in many situations the excessive grid refinement led to Grid Induced Separation (GIS). To overcome this problem, enhancements were proposed leading to new DES variations.

An alternative to DES was proposed by Menter *et al.* (2003) called the Scale-Adaptive Simulation (SAS). SAS is essentially a URANS model, which is capable to resolve turbulent structures in highly separated regions. This is achieved through the usage of the von Karman length scale, which emerges naturally from the model equations, being responsible to adjust the model's behavior to produce a LES-like solution. Although both DES and SAS operate similarly in different

regions of the flow (i.e. the attached boundary layers are solved like in URANS model and the "detached" unsteady-state flow is simulated) the grid spacing does not explicitly influence the URANS model.

In this context, based on the Spalart-Allmaras (SA) turbulent closure model, the present work concerns two hybrid URANS-LES modeling strategies for turbulent flows: the original proposal of DES (SA-DES) and a recently new scale-adaptive model variant (SA-SAS) proposed by Coder (2015). These hybrid URANS-LES modeling methodologies were implemented in the MFSim code, developed in the Laboratório de Mecânica dos Fluidos (MFlab) of the Universidade Federal de Uberlândia (UFU) in partnership with PETROBRAS, and compared with both the dynamic LES model proposed by Germano and the classic SA model. To perform the comparison, simulations were carried out using the configuration of the bluff-body stabilized premixed flame, experimented by Sjunnesson *et al.* (1992).

2. PHYSICAL MODEL

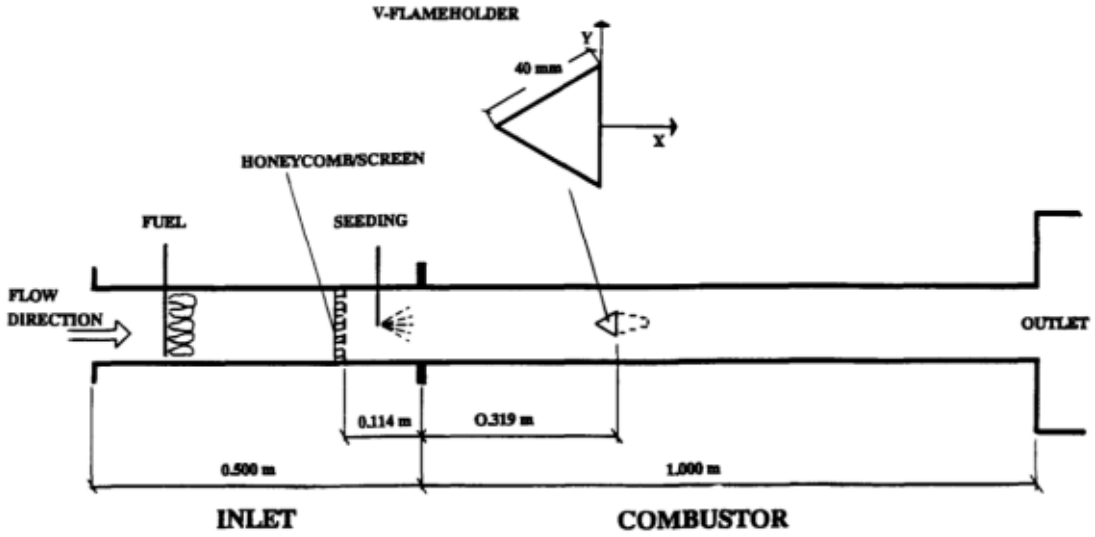

Figure 1. Schematic of the Volvo test rig. Adapted from Sjunnesson *et al.* (1992).

The apparatus consists of a 1.5 m long rectangular duct which is 0.24 m wide by 0.12 m high. It is divided in two sections: the inlet (0.5 m long) and the combustor (1.0 m long). At the inlet section the flow is conditioned by using honeycombs to control the turbulence level. It also contains particle seeding for the LDA measurements and a fuel injector for the reactive cases. A triangular cylinder, with characteristic length of $a = 0.04$ m is mounted 0.682 m upstream from the exit spanning the width of the duct, acting as the bluff-body flameholder.

The experimental data available includes mean and root-mean-square (RMS) velocity data from Laser Doppler Anemometry (LDA) for axial profiles along centerline and transverse profiles across the height of the combustor section at several axial locations, downstream the bluff-body.

The Reynolds number of the flow is $48,000$ based on the characteristic length of the bluff-body, the bulk inlet velocity (U_0) and viscosity at the flow inlet temperature. Inlet turbulence intensity levels are estimate between 3% and 4% (West *et al.*, 2017).

2.1 The computational domain

The computational domain, presented in Fig. 2, mimics the experimental combustor section. Its dimensions are $24a$ x $3a$ x $3a$, where a is the characteristic length of the triangular cylinder. It is important to observe that in the original experiment the domain width was $6a$. The use of $2a$ in the section width together with periodicity condition has been successfully reported by several authors (Wu *et al.*, 2017; Wey, 2017; Sankaran and Gallagher, 2017; Potturi *et al.*, 2017). Thus, the use of $3a$ in the width of the duct together with periodicity condition is not a problem. The value of $3a$, instead of $2a$, was chosen because it defines a more balanced domain for the use of the MFSim code, since it facilitates the work of the Multigrid-Multilevel method. The base mesh is composed of 64 x 8 x 8 volumes, with 4 refinement levels, totalling $1.912.351$ control volumes. The flameholder was modelled by means of a immersed boundary method (Vedovoto *et al.*, 2015).

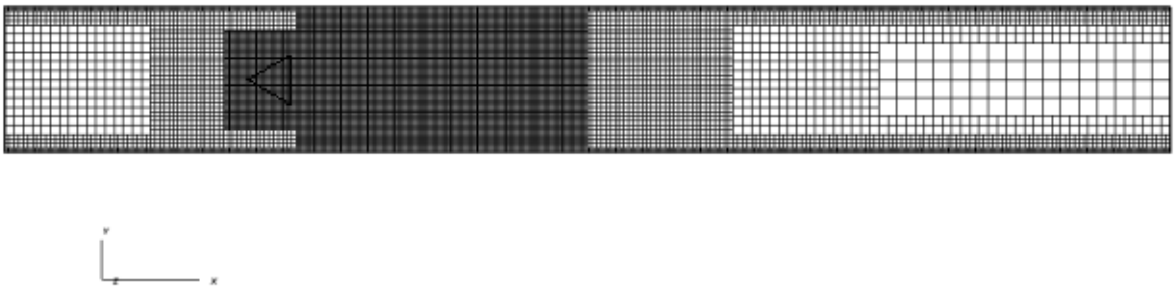

Figure 2. Computational domain used for the simulations.

3. MATHEMATICAL MODEL

In the pursuit of the mathematical model, the following simplifying assumptions are used: (a) fluid is considered as Newtonian, (b) the flow is considered incompressible and (c) isothermal. This leads us to the continuity equation and the Navier-Stokes equations presented below, in their filtered form and in indicial notation:

$$\frac{\partial \tilde{u}_i}{\partial x_i}, \tag{1}$$

$$\frac{\partial \tilde{u}_i}{\partial t} + \frac{\partial}{\partial x_j}\left(\tilde{u}_i \tilde{u}_j\right) = -\frac{1}{\rho}\frac{\partial \tilde{p}}{\partial x_i} + \frac{\partial}{\partial x_j}\left[\nu\left(\frac{\partial \tilde{u}_i}{\partial x_j} + \frac{\partial \tilde{u}_j}{\partial x_i}\right) - \tau_{ij}\right] + \frac{\tilde{f}_i}{\rho}, \tag{2}$$

where $\tilde{u}_i$ are filtered components of the velocity vector, ρ the specific mass, $\tilde{p}$ the filtered pressure, ν the fluid kinematic viscosity, τ_{ij} is the subgrid scale (SGS) stress tensor and $\tilde{f}_i$ an external force. Through the Boussinesq hypothesis, one can write:

$$\tau_{ij} = 2\nu_t \tilde{S}_{ij} - \frac{2}{3}k\delta_{ij}, \tag{3}$$

where ν_t is the eddy viscosity, $\tilde{S}_{ij}$ the filtered strain rate tensor, k the turbulent kinetic energy and δ_{ij} the Kronecker delta. In order to close the system of equations defined by Eqs. (1) and (2) one needs a model to the eddy viscosity. The different approaches used in this work are presented below.

3.1 The Dynamic LES Model

In the Smagorinsky closure model (Smagorinsky, 1963), the eddy viscosity is obtained assuming that the small scales are in equilibrium, which means that the energy production and dissipation balance out in this scales, yielding

$$\nu_t = \left(C_s\Delta\right)^2 \left|\tilde{S}\right| = \left(C_s\Delta\right)^2 \left(2\tilde{S}_{ij}\tilde{S}_{ij}\right)^{1/2}, \tag{4}$$

where Δ is the filter width (which is proportional to the grid size) and C_s denotes the Smagorinsky constant. As presented by Germano *et al.* (1991), a series of tests have been carried out by different authors in order to find the optimum value of C_s. It is shown that even with modifications of the Smagorinsky model, it is not possible to model effectively a variety of phenomena presented in different flows with a single and universal constant.

The dynamic SGS stress model, proposed by Germano *et al.* (1991); Lilly (1992), is an attempt to overcome these deficiencies, in which the Smagorinsky model constant is dynamically computed based on the information provided by the resolved scales of the motion. It is done by applying a second filter to the equations of motion, Eqs. (1) and (2), providing a new way to evaluate the constant used in the Smagorinsky model

$$c\left(\vec{x},t\right) = -\frac{1}{2}\frac{L_{ij}M_{ij}}{M_{ij}M_{ij}}, \tag{5}$$

where the Germano identity, L_{ij}, and the auxiliary tensor, M_{ij}, are defined, respectively, by

$$L_{ij} = T_{ij} - \tau_{ij} \tag{6}$$

and

$$M_{ij} = \widehat{\overline{\Delta}}^2 \left|\widehat{\overline{S}}\right| \widehat{\overline{S}}_{ij} - \overline{\Delta}^2 \widehat{\left|\overline{S}\right|\overline{S}}_{ij}. \tag{7}$$

3.2 The Spalart-Allmaras Model

Spalart and Allmaras (1992) presented a one equation turbulence closure model based on the evaluation of a modified eddy viscosity, $\tilde{\nu}$. Except in regions dominated by viscous effects, $\tilde{\nu}$ equals the eddy viscosity, ν_t. The model was developed using empiricism, arguments based on dimensional analysis, Galilean invariance, in addition to what is called by the authors of selective dependence on molecular viscosity. The models transport equation is given by:

$$\frac{\partial \widetilde{\nu}}{\partial t} + \frac{\partial \left(u_j \widetilde{\nu}\right)}{\partial x_j} = c_{b1}\widetilde{S}\widetilde{\nu} + \frac{1}{\sigma}\left\{\frac{\partial}{\partial x_j}\left[\left(\nu + \widetilde{\nu}\right)\frac{\partial \widetilde{\nu}}{\partial x_j}\right] + c_{b2}\left(\frac{\partial \widetilde{\nu}}{\partial x_j}\right)^2\right\} - c_{w1} f_w \left(\frac{\widetilde{\nu}}{d}\right)^2 \tag{8}$$

A damping function is needed to relate both eddy viscosities as

$$\nu_t = \widetilde{\nu} f_{v1} \tag{9}$$

where

$$f_{v1} = \frac{\chi^3}{\chi^3 + c_{v1}^3}, \tag{10}$$

$$\chi \equiv \frac{\widetilde{\nu}}{\nu}. \tag{11}$$

Additional relations are

$$\widetilde{S} \equiv S + \frac{\widetilde{\nu}}{\kappa^2 d^2} f_{v2}, \qquad f_{v2} = 1 - \frac{\chi}{1 + \chi f_{v1}}, \tag{12}$$

where S is computed as the strain rate $\sqrt{2S_{ij}S_{ij}}$ and d is the distance to the closest wall. Finally, the f_w function is

$$f_w = g\left(\frac{1 + c_{w3}^6}{g^6 + c_{w3}^6}\right)^{\frac{1}{6}}, \qquad g = r + c_{w2}\left(r^6 - r\right), \qquad r \equiv \frac{\widetilde{\nu}}{\widetilde{S}\kappa^2 d^2}. \tag{13}$$

The closure coefficients for the model are: $c_{b1} = 0,1355$, $\sigma = 2/3$, $c_{b2} = 0,622$, $\kappa = 0,41$, $c_{w1} = c_{b1}/\kappa + (1 + c_{b2})/\sigma$, $c_{w2} = 0,3$, $c_{w3} = 2$, $c_{v1} = 7,1$, $c_{t1} = 1$, $c_{t2} = 2$, $c_{t3} = 1,1$ and $c_{t4} = 2$.

3.3 The Spalart-Allmaras DES Model

Starting from the original SA model, the SA-DES model can be reached by replacing the distance to the wall, d, by a modified distance to the wall, $\tilde{d}$, given by

$$\widetilde{d} \equiv min\left(d, C_{DES}\Delta\right), \tag{14}$$

where Δ is defined by

$$\Delta \equiv max\left(\Delta x, \Delta y, \Delta z\right), \tag{15}$$

and C_{DES} is a constant calibrated through the Decaying of Homogeneous Isotropic Turbulence (DHIT) experiments. In the present work, $C_{DES} = 0.65$ as recommended by Shur *et al.* (1999).

3.4 The Spalart-Allmaras SAS Model

Coder (2015) presented a scale-adaptive variation of the SA model, derived from the original two equations SAS model presented by Menter *et al.* (2003). The only difference from the new model to the original SA model is the inclusion of a new source term in the transport equation, given by

$$Q_{SAS} = -c_{s1} max\left(\frac{\kappa^2}{L^2} - \frac{c_{s2}}{d^2}, 0\right)\widetilde{\nu}^2, \tag{16}$$

with

$$L = max\left(L_{vK}, \kappa C_{DES}\Delta\right), \tag{17}$$

and

$$L_{vK} = \kappa \frac{S}{\sqrt{\frac{\partial^2 u_i}{\partial x_m^2}\frac{\partial^2 u_i}{\partial x_n^2}}}. \tag{18}$$

The constants $c_{s1} = 4.90$, $c_{s2} = 2.00$ and $C_{DES} = 0.65$ follows the authors recommendations. Here the mesh characteristic length, Δ, was used as a limiting factor for the von Karman length scale.

4. RESULTS AND DISCUSSIONS

In order to evaluate the models, three different axial locations downstream of the bluff-body are considered for comparison with experimental measurements. Mean axial velocity profiles are shown in Fig. 3a. At the axial location $x/a = 0.375$ the behavior of the four models is very similar. The wake momentum deficit region was underestimated by all models. However, better agreement is observed with the SA and SA-SAS models. At the next axial location $x/a = 1.53$, a slow diffusion process of the SA and LES-D models is detected, while a better agreement was obtained by the SA-DES and SA-SAS models. For the last axial location $x/a = 3.75$, difficulties in the diffusion process of all models can again be observed. The SA model continues to show low diffusion, while the other models exhibited a more widespread velocity profile than the experimental one. Mean transverse velocity profile are also presented by Fig. 3c. Good agreement can be observed at all three axial locations, except at $x/a = 1.53$, where the experiments have larger magnitude at the upper half of the domain.

The root-mean-square axial velocity (u-RMS) profiles is shown in Fig. 3b. At the first axial location $x/a = 0.375$, it is not possible to correctly capture this quantity inside the wake momentum deficit region. Although good agreement can be observed outside the refereed region, the u-RMS magnitude is underestimated inside the wake momentum deficit region, specially by LES-D and SA-DES models. It is observed that the use of the SA-SAS model enabled a better result. This discrepancies from the experimental results suggest that different boundary conditions may be employed in the current simulation to that in the experiments, e.g. the flow is assumed to be laminar at the inlet. Although this is usually a good assumption in this case - once the turbulence level is controlled inside the experimental test rig - inlet turbulence conditions may be necessary to correctly predict u-RMS values.

At the second axial location, good agreement is obtained for the u-RMS values at the lower half of the domain. The same behavior was observed by Menter and Egorov (2010), indicating a possible error in the measurement of the data during the material experiment. At the axial location $x/a = 3.75$ similar behavior of the SA-DES and SA-SAS models is observed, while the LES-D model shows a better agreement with experiments.

The root-mean-square transverse velocity (v-RMS) profiles are also presented in Fig. 3d. The behavior at the first axial location $x/a = 0.375$, is similar to that observed at the same location in Fig. 3b. Both LES-D and SA-DES models underestimated the v-RMS values, while the SA-SAS shows excellent agreement. At the next two locations $x/a = 1.53$ and $x/a = 0.375$, all models presented similar results. It is worthy to mention that at location $x/a = 0.375$ the simulations shows a less widespread v-RMS profile than observed in the experimental data, but it also shows an averaged flow field symmetrical with respect to the domain centerline, as it should be.

The LES-D, SA-DES and SA-SAS models were able to capture, at the three measurement stations, the trends of the Reynolds stress tensor, $\overline{u'v'}$, as shown in Fig. 5. The largest difference was observed, again, in the first measuring station. Note that the $\overline{u'v'}$ was underestimated using the LES-D and SA-DES models, in regions close to $y = \pm 0.5$. A better agreement with the experimental data was observed with the SA-SAS model.

The last comparison with experimental data presents results for two more quantities as well for the axial velocity at the centerline of the domain downstream the bluff-body. The anisotropy and the fluctuation level are defined as V_{RMS}/U_{RMS}

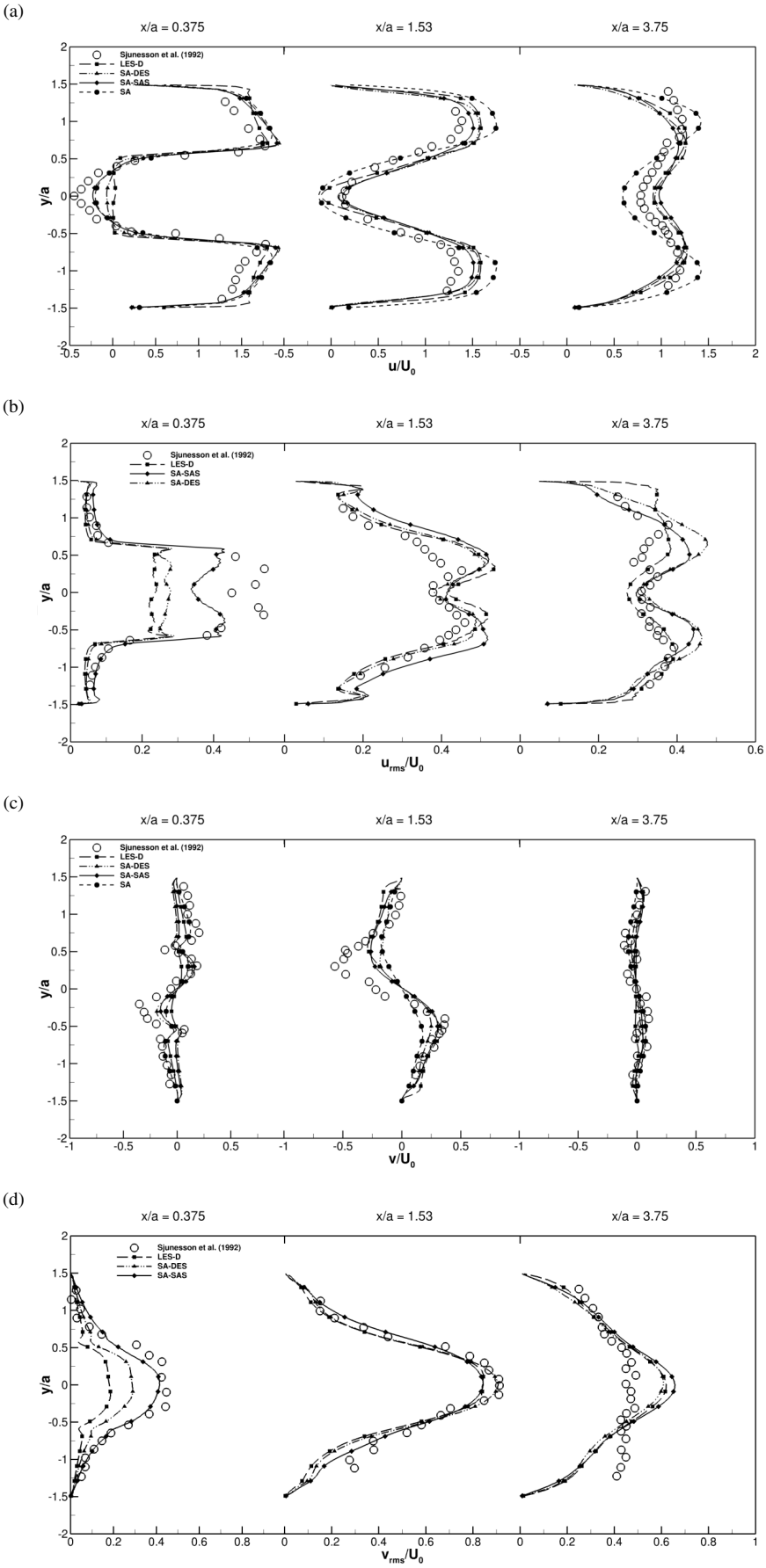

Figure 3. Velocity profiles and turbulence RMS profiles for three different stations downstream of the triangular cylinder (x/a=0.375, x/a=1.53, x/a=3.75). Comparison of LES-D, SA-DES, SA-SAS, SA models and experiment (**a** U-velocity, **b** u_{rms}, **c** V-velocity, **d** v_{rms}).

(a)

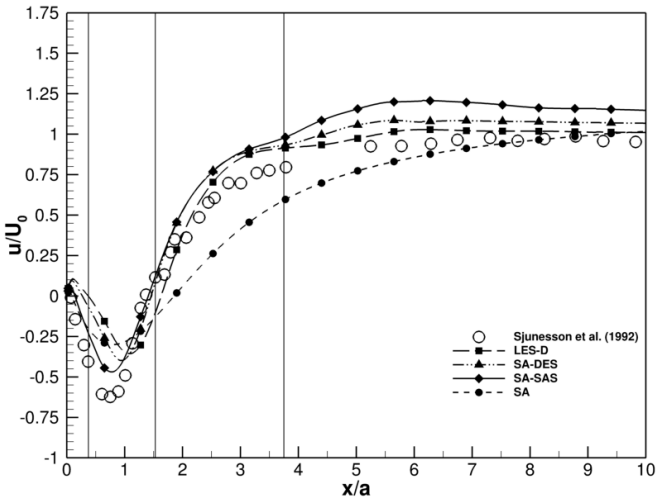

(b)

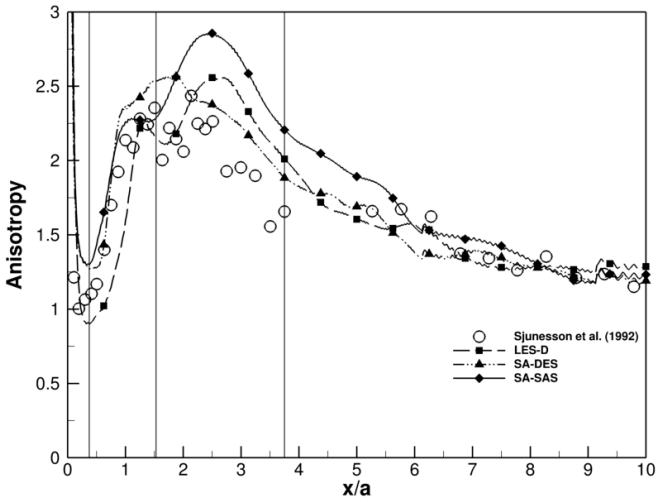

(c)

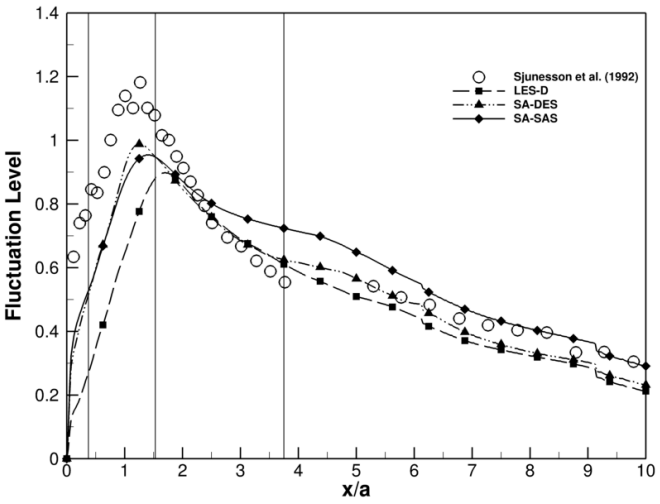

Figure 4. Centerline profiles for (a) mean axial velocity, (b) anisotropy and (c) fluctuation level downstream of the triangular cylinder. Comparison of LES-D, SA-DES, SA-SAS, SA models and experiment.

and $\sqrt{U_{RMS}^2 + V_{RMS}^2}/U_0$, respectively. Figure 4 shows the results from simulations using the models considered. The three vertical lines highlight the axial locations downstream of the bluff-body where the results presented in Fig. 3 were extracted. The results for the axial velocity of LES-D, SA-DES and SA-SAS models exhibits little difference until the axial location $x/a = 3.75$, where they begin to differentiate from each other. All three overpredict the axial velocity after the refereed location. The SA model in turn underpredicted the axial velocity between the axial locations $x/a = 1.53$ and $x/a = 3.75$.

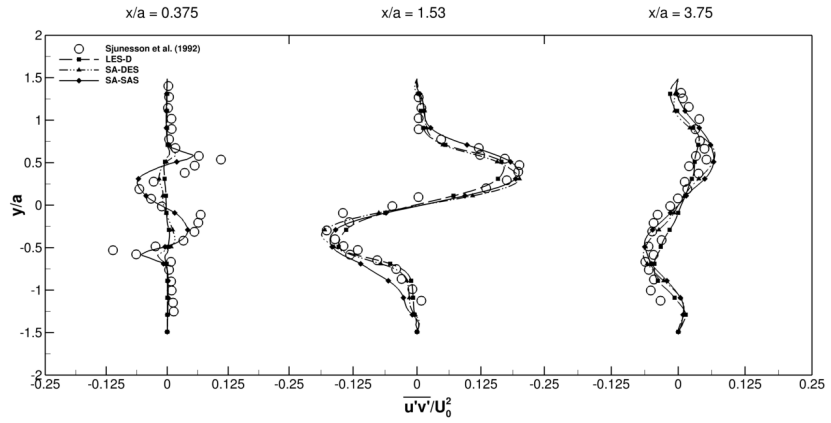

Figure 5. Reynolds stress profiles for three different stations downstream of the triangular cylinder (x/a=0.375, x/a=1.53, x/a=3.75). Comparison of LES-D, SA-DES, SA-SAS, SA models and experiment.

The anisotropy profiles also shows discrepancies for the three models simulated between the axial locations $x/a = 1.53$ and $x/a = 3.75$, while the fluctuation level exhibits good agreement, except by axial locations before $x/a = 2.0$. This last discrepancy from the experimental measurements corroborates with the idea that more informations about turbulence at the inlet are needed to correct predict the flow, specially with LES-like models, as seen in Fig. 3b.

5. CONCLUSIONS

A series of simulations were performed for the Volvo bluff-body stabilized combustion configuration using four turbulence closure models. Only the non-reacting case is calculated. The dynamic LES model was compared with the Spalart-Allmaras URANS model and two hybrid methodologies based on the Spalart-Allmaras model: the Detached-Eddy Simulation and Scale-Adaptive Simulation. The hybrid methodologies were implemented in the MFSim code, developed in the Laboratório de Mecânica dos Fluidos of the Universidade Federal de Uberlândia in partnership with PETROBRAS.

Mean velocity profiles and turbulence RMS profiles were compared with experimental data and showed good agreement. It was observed that a better agreement for the turbulent RMS could be achieved by introducing a more realistic turbulent boundary condition at the inlet, specially for the Large Eddy Simulations were a completely lack of turbulence information is experimented. For the hybrid models a reference turbulent intensity of 3.5% was used to estimate the boundary conditions for the transported variables. This may have masked the results since the Large Scale Simulation presented inferior performance to the studied hybrid models, even being able to solve a bigger part of the spectrum of turbulent structures. A closer investigation of this aspect is the subject of future research.

The hybrid methodologies, specially the SA-SAS model, proved to be interesting alternatives when dealing with turbulent flow simulations within the MFSim code. Further investigations regarding CPU efficiency and a wider range of test cases are also subject of future research.

6. ACKNOWLEDGEMENTS

The authors are greatful to FAPEMIG, CAPES and PETROBRAS for providing financial support.

7. REFERENCES

Coder, J.G., 2015. "A scale-adaptive variant of the spalart-allmaras eddy-viscosity model". *AIAA-2015-2462*.

Germano, M., Piomelli, U., Moin, P. and Cabot, W.H., 1991. "A dynamic subgridscale eddy viscosity model". *Phys. Fluids A*, Vol. 3, pp. 1760–1765.

Haase, W., Braza, M. and Revell, A., 2009. "Desider - a european effort on hybrid urans-les modelling". In *Notes on Numerical Fluid Mechanics and Multidisciplinary Design*. Springer Berlin Heidelberg.

Lilly, D.K., 1992. "A proposed modification of the germano subgrid-scale closure model". *Phys. Fluids A*, Vol. 4, pp. 633–635.

Menter, F.R. and Egorov, Y., 2010. "The scale-adaptive simulation method for unsteady turbulent flow predictions. part 1: Theory and model description". *Flow Turbulence Combust*, Vol. 85, pp. 113–138.

Menter, F.R., Kuntz, M. and Bender, R., 2003. "A scale-adaptive simulation model for turbulent flow predictions". *AIAA-2003-0767*.

Peng, S.H., Doerffer, P. and Haase, W., 2010. "Progress in hybrid rans-les modelling". In *Notes on Numerical Fluid Mechanics and Multidisciplinary Design*. Springer Berlin Heidelberg.

Potturi, A.S., Patton, C.H. and Edwards, J.R., 2017. "Advanced les models for turbulent combustion". In *Proceedings of the 55th AIAA Aerospace Sciences Meeting*. Grapevine, Texas.

Sankaran, V. and Gallagher, T.P., 2017. "Grid convergence in les of bluff body stabilized flames". In *Proceedings of the 55th AIAA Aerospace Sciences Meeting*. Grapevine, Texas.

Shur, M., Spalart, P.R., Strelets, M. and Travin, A., 1999. "Detached-eddy simulation of an airfoil at high angle of attack". In *Proceedings of the 4th International Symposium on Engineering Turbulence Modelling and Measurements*. Corsica.

Sjunnesson, A., Henriksson, R. and Lofstrom, C., 1992. "Cars measurements and visualization of reacting flows in bluff body stabilized flame". *AIAA-92-3650*.

Smagorinsky, J., 1963. "General circulation experiments with the primitive equations. i. the basic experiment". *Month. Wea. Rev.*, Vol. 91, p. 99âĂŞ164.

Spalart, P.R. and Allmaras, S.R., 1992. "A one-equation turbulence model for aerodynamic flows". *AIAA-92-0439*.

Spalart, P.R., Jou, W.H., Strelets, M. and Allmaras, S.R., 1997. "Comments on the feasibility of les for wings, and on a hybrid rans-les approach". In *Proceedings of the 1st Advances in DNS-LES: Direct numerical simulation and large eddy simulation*. Ruston, LA.

Vedovoto, J.M., Serfaty, R. and Silveira-Neto, A., 2015. "Mathematical and numerical modeling of turbulent flows". *An. Acad. Bras. CiÃłnc.*, Vol. 87, pp. 1195–1232.

West, J.P., Groth, C.P.T. and Hu, J.T.C., 2017. "Application of detached eddy simulation to a bluff body flame stabilizer in duct flow". In *Proceedings of the 55th AIAA Aerospace Sciences Meeting*. Grapevine, Texas.

Wey, T., 2017. "Model validation for propulsion - on the tfns and les subgrid models for a bluff body stabilized flame". In *Proceedings of the 55th AIAA Aerospace Sciences Meeting*. Grapevine, Texas.

Wu, H., Peter, C.M., Yu, L. and Ihme, M., 2017. "MVP-workshop contribution: Modeling of volvo bluff flame experiment and comparison of finite-volume and discontinuous-galerkin schemes". In *Proceedings of the 55th AIAA Aerospace Sciences Meeting*. Grapevine, Texas.

8. RESPONSIBILITY NOTICE

The authors are the only responsible for the printed material included in this paper.